Voxel-wise analysis of paediatric liver MRI

Ged Ridgway[1], Kamil Janowski[2], Andrea Dennis[1], Velicia Bachtiar[1], John McGonigle[1], Chris Everitt[3], Angela Darekar[3], David Breen[3], Dan Green[1], Stefan Neubauer[1], Rajarshi Banerjee[1], Piotr Socha[2], and Sir Michael Brady[1]

[1] Perspectum Diagnostics Ltd, Oxford, UK
[2] The Children's Memorial Health Institute, Warsaw, Poland
[3] University Hospital Southampton NHS Foundation Trust, Southampton, UK

Abstract. Paediatric liver disease is a growing problem, which would benefit from non-invasive techniques for early detection and treatment monitoring. Multiparametric quantitative MRI has shown promise for measuring liver steatosis, inflammation and fibrosis in adults, but is likely to need modification for children. The Kids4LIFe project (NCT03198104) aims to adapt and validate Liver*MultiScan*™ from Perspectum Diagnostics for paediatric applications, characterising healthy liver development and a range of diseases. The analysis of Liver*MultiScan*™ images usually focuses on a few regions of interest, or on distributional features of the segmented liver parenchyma. The present work is an initial investigation into the use of voxel-wise statistical analysis in atlas space, following nonlinear image registration, with the aim of localising effects (developmental or disease-related), as commonly done in neuroimaging. Preliminary results show statistically significant effects that warrant further characterisation, and suggest atlas-based analysis is a useful complement to current approaches.

1 Introduction

Paediatric liver diseases are 'silent killers' as clinical symptoms only surface late in the disease course. Incidence rates of obesity and paediatric non-alcoholic fatty liver disease (NALFD) are fast-growing in Europe, and higher still in the USA [6], associated with several health risks and a substantial economic burden.

Current techniques for the diagnosis and monitoring of liver disease are either insensitive (blood tests, ultrasound) or invasive, risky, costly and topographically limited (biopsy from a tiny fraction of liver). Ultrasound-based methods often fail in obese children and don't detect disease at an early stage. Biopsy is generally considered to be unacceptable for asymptomatic children. Thus, there is an urgent need to develop methods that can assess liver disease non-invasively at an early stage and are applicable for the millions of obese children worldwide [6].

Perspectum Diagnostics' multiparametric Liver*MultiScan*™ has FDA 510(k) clearance for assessing liver disease in adults. In particular, iron-corrected longitudinal relaxation time (cT1) correlates with fibrosis and inflammation measured with biopsy [2], and predicts clinical outcomes [7]. However, liver disease in children can differ from adults in aetiology, natural history and pathological

findings. The Kids4LIFe project aims to develop Liver*MultiScan*™ for paediatric applications, to assess healthy childhood development and disease.

In this paper, we explore the utility of voxel-wise statistical analysis following nonlinear registration to a group-wise average atlas, as is common in the field of neuroimaging. Initial results suggest relatively subtle developmental effects, and promising but preliminary characterisation of disease.

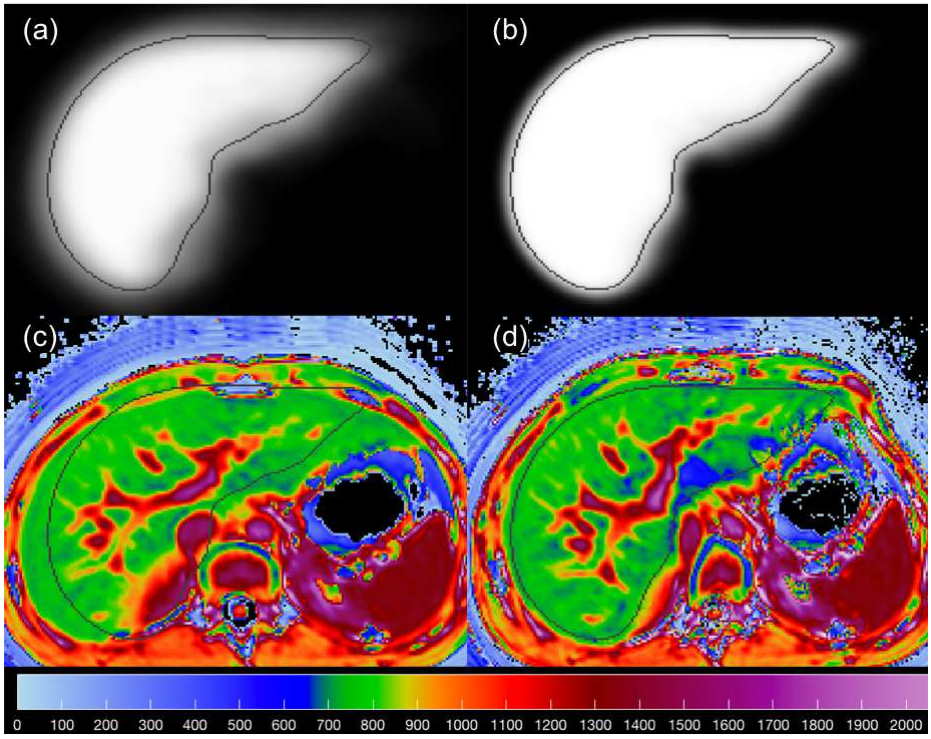

Fig. 1. Atlas building. (a) Initial average of centroid-aligned masks. (b) Final average of non-linearly warped masks (contour at 0.8 of this image defines the analysis mask, shown on all similar images). (c) Example centroid-aligned case. (d) Same example case non-linearly warped. The colour-scale shows standardised cT1 in ms.

2 Methods

Patients and healthy controls were recruited at the Children's Memorial Health Institute (CZD) in Warsaw, Poland, where they were scanned on a 1.5 T Siemens Avanto$^{\text{fit}}$. Additional healthy volunteers were scanned at two sites in the UK: University Hospital Southampton NHS Foundation Trust (UHS), on a 3 T Siemens

Skyra; and Imanova in London, on a 3 T Siemens Verio. Clinical data were stored and transferred using systems developed by Silvermedia[4].

The Liver*MultiScan*™ protocols and modelling provide maps of quantitative T_1 and T_2^* and proton-density fat-fraction (PDFF). A corrected T1 (cT1) is derived to account for the influence of iron on the longitudinal relaxation, and standardised to account for differences between scanners. These standardised cT1 maps are the focus of the present study. Four 8mm thick slices with in-plane resolution of 1.1 mm are acquired approximately 10–15 mm apart. The slices are stacked into a 'pseudo-volume' (voxel-size 1.1 by 1.1 by slice-separation), to enable the registration procedure to attempt to account for variation in slice positioning.

Liver masks were defined on cT1 slices by a trained operator. Images were stacked into pseudo-volumes, then translated such that the mask centroid became the origin. Masks were resampled to 1mm isotropic and smoothed with a 6mm full-width at half-maximum (FWHM) Gaussian kernel. These smoothed masks were then iteratively warped to an evolving estimate of their group-wise average using the large-deformation diffeomorphic registration approach [1] in the SPM12 'Shoot' toolbox.[5] The resultant average template was thresholded at a level of 0.8 to define a binary analysis mask for the voxel-wise statistical modelling. The cT1 images were transformed to atlas space. The approach is illustrated in Fig. 1.

The warped cT1 images were smoothed with a 6mm FWHM Gaussian kernel using a normalised convolution procedure [5] over the analysis mask, such that boundary effects are avoided. The smoothed cT1 images were then analysed in a voxel-wise mass-univariate manner [4]. SPM12 was used to fit voxel-wise linear models and to assess the significance of effects while correcting for multiple testing over many spatially dependent voxels using random field theory [3] to control the family-wise error rate (FWE).

One model was fitted in the healthy controls, comprising the interaction of age and sex (i.e. allowing different linear aging trajectories in boys and girls) and a factor to adjust for differences between scanning sites. A second model was fitted to controls and patients (pooling all diagnoses), adjusting for (non-interacting) age and sex; it was not practical to adjust for site in this model due to the severe imbalance of diagnosis by site (discussed later). A third model similar to the second looked only at the largest single diagnostic group: autoimmune hepatitis (AIH). A series of models were then fitted in patients, each model comprising one measure of interest from the liver biopsy, alongside terms for age and sex.

3 Results

Demographic data are summarised in Table 1; the relatively high number of subjects excluded (22/102) reflects the challenges of acquiring MRI in children. The balance of male and female subjects does not differ across sites (Fisher's exact test $p>0.5$). Age differs significantly across sites (Kruskall-Wallis $p=0.0165$), but not between controls and patients ($p > 0.1$). The most common disease diagnosis

[4] Kraków, Poland, `https://silvermedia.pl/en/`

[5] SPM12 revision 7219, `http://www.fil.ion.ucl.ac.uk/spm`, under MATLAB R2017a.

was AIH. Other cases included an additional 5 with suspected AIH, 6 mixed AIH with primary sclerosing cholangitis (PSC), and 4 with Wilson's disease.

Table 1. Demographic data. All columns after the second relate to the analysed subset.

Site	Recruited	Analysed	Female	Age ($\mu \pm$ sd yr)	Healthy	AIH	Other
CZD	66	50 (76%)	28 (56%)	13.0 ± 3.5	4	26	20
Imanova	9	8 (89%)	4 (50%)	13.9 ± 3.9	8		
UHS	27	22 (81%)	13 (59%)	10.8 ± 2.7	22		
Total	102	80 (78%)	45 (56%)	12.5 ± 3.4	34		

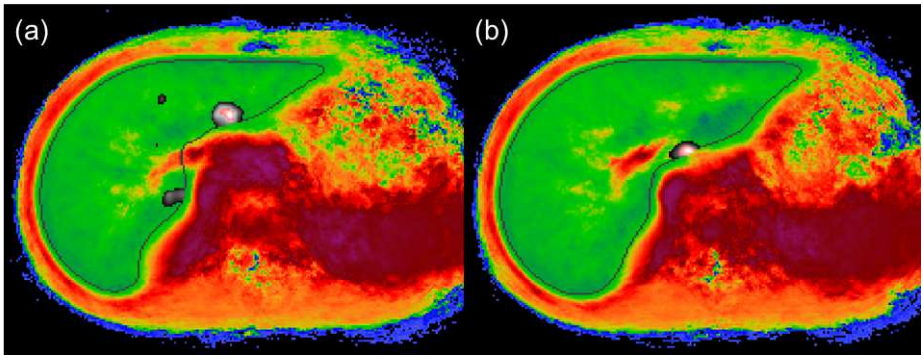

Fig. 2. Example results within healthy controls. (a) Increasing cT1 with age in girls; axial slice 6mm below template centre. (b) Differences in cT1 across sites; axial slice 1mm above template centre. Significant effects are shown in pink after correction for multiple testing (pFWE < 0.05) with uncorrected results ($p < 0.001$) shown in greyscale for further context. Background cT1 is on the same colour-scale as Fig. 1.

Figure 2 shows results from the modelling of developmental trajectories in healthy controls. There are two significant regions with increasing cT1 associated with age in girls; however, due to the relatively small sample size, we are unable to demonstrate analogous significant (corrected for multiple testing) increases in boys, or to conclude that the regression slope of cT1 on age is steeper in girls than boys. There is a single significant region for the effect of site, close to the edge of the analysis mask.

Compared to healthy controls, Fig. 3 shows widespread differences for the patients (pooling all diagnoses), together with more localised effects for the smaller but homogeneous group of AIH patients.

Within the group of 44 patients with biopsy data available, Fig. 4 shows a single region with significant (corrected) correlation of cT1 with Ishak fibrosis,

and extensive correlation (10 regions, of which 6 are visible on the illustrated slice) between cT1 and ballooning degeneration.

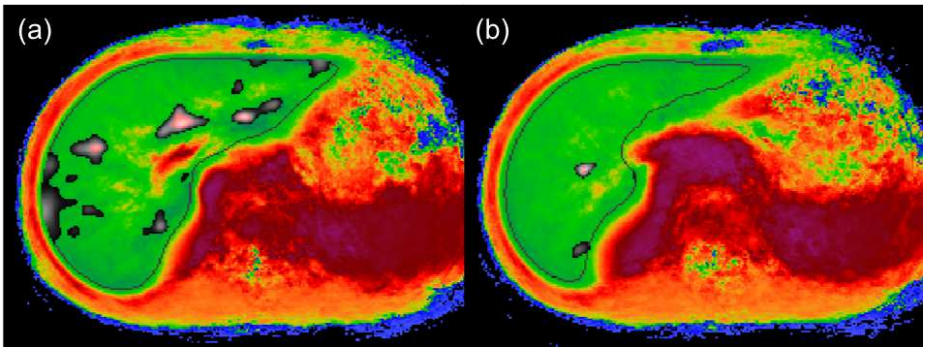

Fig. 3. Group comparison of patients and controls. (a) Significantly greater cT1 (pink, pFWE<0.05; grey, uncorrected p<0.001) for all pooled patients (n=46) vs controls (n=34). Axial slice at template centre. (b) Significantly greater cT1 for AIH patients (n=26) vs controls. Axial slice 10mm below template centre.

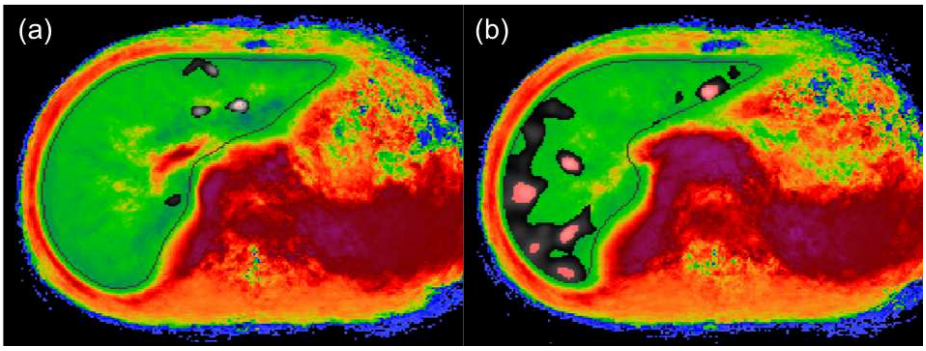

Fig. 4. Correlations with biopsy measurements in patients. (a) Significant correlation (pink, pFWE<0.05; grey, uncorrected p<0.001) of cT1 with Ishak fibrosis. Axial slice 1mm below template centre. (b) Significant correlation of cT1 with ballooning degeneration. Axial slice 9mm below template centre.

4 Discussion

The preliminary results raise interesting questions (for example whether the increase in cT1 with age in girls relates to the effects of puberty) but require more extensive characterisation in a larger sample.

The chief limitation with the current dataset is the serious imbalance of diagnosis across sites, as shown in Table 1. This doesn't affect the results within controls or patients separately (Figs. 2 and 4) but means that the comparisons between controls and patient groups (Fig. 3) must be interpreted very cautiously, as no significant regions remained when adjusting for site. Additional healthy controls continue to be acquired at CZD, though there are currently no plans to acquire patient data at the two UK sites. It is of some reassurance that the effects of site in Fig. 2 were limited, but given the small number of analysed controls from CZD, this cannot rule out a substantive effect.

Vessels have high cT1, and the fraction of the liver occupied by vessels differs across diseases. Here, we allow this effect to be exhibited in the analysis, by including vessels within the (atlas-space) mask used for smoothing and analysis. In future work, we plan to perform an additional analysis, with the normalised convolution applied in native space at the subject level with masks that exclude the major vessels, so that we may disambiguate the effects of disease on vessels and on the liver parenchyma. Future work will also extend the approach, developed here for T_1, to the analysis of T_2^* and PDFF.

Acknowledgments

This study was funded by a grant from EU – EUROSTAR project Σ! – Kids4LIFe.

References

1. Ashburner, J., Friston, K.J.: Diffeomorphic registration using geodesic shooting and Gauss-Newton optimisation. NeuroImage 55, 954–967 (Apr 2011)
2. Banerjee, R., Pavlides, M., Tunnicliffe, E.M., Piechnik, S.K., Sarania, N., Philips, R., Collier, J.D., Booth, J.C., Schneider, J.E., Wang, L.M., Delaney, D.W., Fleming, K.A., Robson, M.D., Barnes, E., Neubauer, S.: Multiparametric magnetic resonance for the non-invasive diagnosis of liver disease. Journal of hepatology 60, 69–77 (Jan 2014)
3. Flandin, G., Friston, K.J.: Analysis of family-wise error rates in statistical parametric mapping using random field theory. Human brain mapping (2017)
4. Friston, K., Ashburner, J., Kiebel, S., Nichols, T., Penny, W.: Statistical parametric mapping: the analysis of functional brain images. Academic Press (2007)
5. Knutsson, H., Westin, C.F.: Normalized and differential convolution. In: Proc. IEEE Conf. Computer Vision and Pattern Recognition. pp. 515–523 (Jun 1993)
6. NCD Risk Factor Collaboration (NCD-RisC): Worldwide trends in body-mass index, underweight, overweight, and obesity from 1975 to 2016: a pooled analysis of 2416 population-based measurement studies in 128.9 million children, adolescents, and adults. The Lancet 390, 2627–2642 (2017)
7. Pavlides, M., Banerjee, R., Sellwood, J., Kelly, C.J., Robson, M.D., Booth, J.C., Collier, J., Neubauer, S., Barnes, E.: Multiparametric magnetic resonance imaging predicts clinical outcomes in patients with chronic liver disease. Journal of hepatology 64, 308–315 (Feb 2016)